Cumhuriyet Science Journal
e-ISSN: 2587-246X
ISSN: 2587-2680
Cumhuriyet Sci. J., 42(2) (2021) 502-507
http://dx.doi.org/10.17776/csj.893653

Investigation of deformation and element diffusion in joint interface of mild carbon steel and HCrWCI welded by friction welding

Tanju TEKER [1], *Mustafa ÖZASLAN* [2,*]

[1]*Sivas Cumhuriyet University, Faculty of Technology, Department of Manufacturing Engineering, 58140, Sivas / TURKEY.*
[2]*Körfez Vocational and Technical Anatolian High School, 41780, Körfez, Kocaeli / TURKEY.*

Abstract

In this study, continuous drive friction welding process is selected for joint dissimilar high chromium white cast iron and mild carbon steeel. The microstructure, presence and diffusion of elements, deformation in interface of weld metal were analyzed by scanning electron microscopy (SEM), optical microscopy (OM), energy dispersive spectroscopy (EDS), elemental mapping and X-Ray diffraction (XRD). Elemental analysis was applied to the fractured surface after the tensile test. The rotational speed from the friction welding process parameters had a significant impact on the quality of the welded joint. Due to element diffusion at the weld interface, carbides consisting of Cr_7C_3 and $Cr_{23}C_6$ were occurred. Carbon, which is the dominant element of the diffusion process, was decisive in the emergence of the carbide layer.

Article info

History:
Received: 09.03.2021
Accepted:15.06.2021

Keywords:
HCrWCI,
Mild carbon steel,
Friction welding,
Elemental mapping,
EDS.

1. Introduction

Basically, welding processes are divided into two groups as solid-state welding and fusion welding. In the fusion welding technique, there is a full melting in the weld interface while there is a partial melting in the solid-state welding technique. Due to metallurgical and thermal incompatibility and differences in their melting temperature, melting welding methods may be possible to join alloys by welding [1-3]. Friction welding (FW) is more preferred than other methods in combining different alloys with solid state technique. In this method, the welding interface is heated by the combined effects of the pressure and relative motion of the alloy rods to be joined. The combination of materials is achieved by the plastic deformation of the material [4-6]. It is widely used in the automotive and aerospace industrial.

FW consists of several stages. In the first stage, after the two parts touch each other, friction begins to occur on the opposite interfaces of the parts to be joined. At this stage, the peripheral speed of the moving part is kept constant and friction force is applied to form a metallurgical bond between the parts during friction. Thus, it is allowed to establish a connection by providing element transitions between the contacting parts. In the meantime, local connections occur between the contact surfaces of the parts. These local associations and separations continue as long as the friction movement continues. At this stage, the torque value reaches its maximum value [7-9].

With the advancing engineering technology, material groups that do not have circular symmetry and rotational symmetry, hollow or solid tubular materials can be easily welded with the FW method. Ma et al. reported that the different metal connection between AISI 304 and 1045 grade can be achieved by FW. The joining conditions changed the tensile features of the joint by affecting the density of the carbides at the weld interface and the heterogeneous microstructure in the thermo-mechanically affected zone on the AISI 1040 side [10].

High chromium white cast iron (HCrWCI) has been used in various mineral drilling, leveling, processing spindles, brick molds and processing hard rocks [11, 12]. Since the carbon steels are difficult to weld with fusion welding due to their low weldability [13].

In this study, mild carbon steel and high chrome white cast iron are joined by friction welding method using various rotational speeds. The microstructure, presence and diffusion of elements, deformation in interface of weld metal were analyzed.

2. Materials and Methods

In this study, 75 mm long and 10 mm diameter, HCrWCI (3.2%C, 1.16%Si, 2.3%Mn, 27.4%Cr, 0.5%Ni, 2.3%Mo and Bal.%Fe) and mild carbon steel

*Corresponding author. *e-mail address: mustafa_044@yahoo.com*

(0.41%C, 0.2%Si, 0.8%Mn and Bal.%Fe) were used. The parameters used in the friction welding tests are given in Table 1.

To examine the phases formed in the samples after FW; mild carbon steel side using Nital (2% HNO_3 + 98% Ethanol) solution, HCrWCI side with Vilella solution was etched for 15-20 s. Microstructural properties and deformation, fracture surface morphology, elemental distributions throughout the interface of weld metal were detected through scanning electron microscopy (SEM: ZEISS EVO LS10), energy dispersive spectroscopy (EDS), optical microscope (OM) and elemental mapping. Phase determinations were carried out by Rigaku X-ray diffractometer (XRD) device with CuKα radiation. After the tensile test, fracture surface elemental mapping analysis was performed.

Table 1. Parameters of the joining process made by friction welding method.

Sample	Rotational Speed (rpm/min.)	Friction Time (s)	Friction Pressure (MPa)	Forging Pressure (MPa)	Forging Time (s)
S1	1600	12	80	150	12
S2	1700	12	80	150	12
S3	1800	12	80	150	12

3. Experimental Results

3.1. Macrograph of the welded joints

The surface macro photographs of S1-S3 welded joints combined using different friction speeds (1600, 1700, 1800 rpm) are shown in Fig. 1. Welded joints without pores and cracks were obtained due to the extreme cooling rate after FW. Significant differences were detected in the quantities of flanges formed with increasing rotational speed [14]. In addition, the flashes formed in the welded joints were in the form of a bowl as stated in the literature. The high rotation speed caused a rapid warming up to high temperatures at the interface. Due to the temperature gradient, the axial shortening and the proportion of viscous material pushed out of the interface increased. Thermal features were effective in determining which material deforms preferentially in dissimilar metal joint. If the thermal dissipation of one metal was less than the other, then the temperature would increase within a shorter distance of that part of the joint. Even if the strength of the metal with lower thermal dissipation is very high, it will show more deformation. Although a base material has almost the same properties at room temperature, it begins to lose strength faster as the temperature rises, resulting in a higher rate of flash. As the period of cycles increased, the sample lengths shortened.

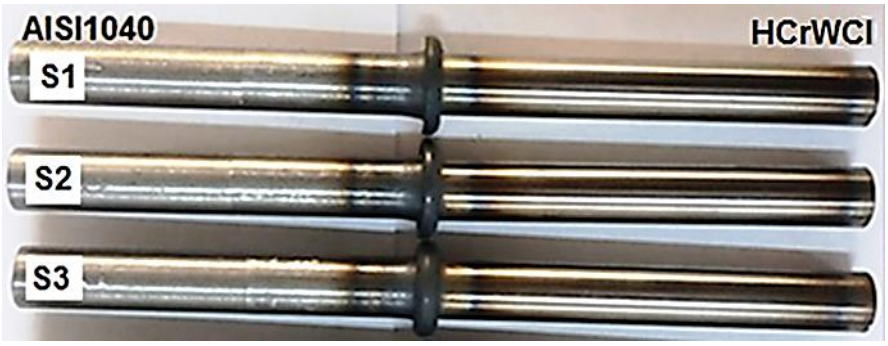

Figure 1. The surface macro photographs of S3 sample.

The view of the regions under thermomechanical interaction is given in Fig. 2. On the HCrWCI side of the welded samples, a narrower thermo-mechanically heat-affected zone was formed compared to the AISI 1040 side. During friction welding, the heat increase caused by friction started from the weld interface and progressed to the base metals. Since the HCrWCI side had a lower thermal conduction coefficient compared to the AISI 1040 side, the heat increase on the HCrWCI side spreads less per unit time. Therefore, the thermo-mechanically heat affected zone on the AISI1040 side was larger.

3.2. Microstructure of joint interface

Optical and SEM photograph of S3 sample is given in Fig. 3. The microstructure of the joint interface generally displayed a similar appearance.

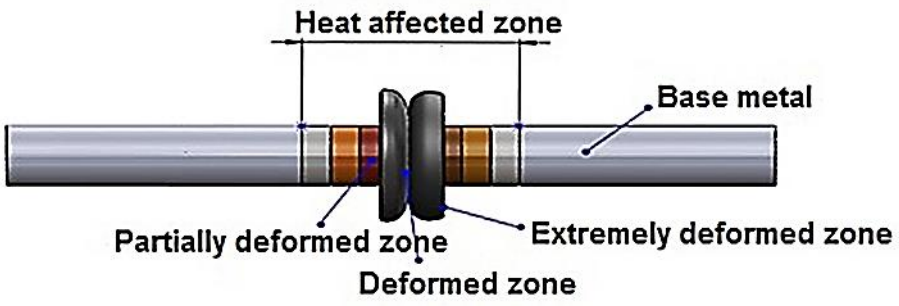

Figure 2. The view of the regions under thermomechanical interaction.

As stated in the literature, it was determined that four different regions were formed in welded joints. These regions are the extremely deformed zone (EDZ), deformed zone (DZ), partially deformed zone (PDZ) and the base metal (BM), respectively [15-17]. The grains of weld zone were thinner than the PDZ. The joint zone reached the highest temperature, which was below the solidus temperature. This led to the growth of ferrite grains. Due to the fully dissolution of austenite in heating, ferrite increased the austenite ratio. The distinction between the maximum temperature obtained at the weld pool and the room temperature at the period of cooling caused in the rise of the cooling amount. Diffusional conversion to the austenite phase was limited by the cooling leading to the dominant ferrite structure in the weld seam [18]. A thin layer of proutectoid ferrite consisted and was adjacent to the weld interface on AISI 1040 sides both in the central zone and in the peripheral zone. Lesser ferrite and rough pearlite grains accumulated in the pearlite grain boundaries. Frictional temperature and plastic distortion provided thinning and recrystallization of milled austenite grains induced by mechanical friction at the weld interface.

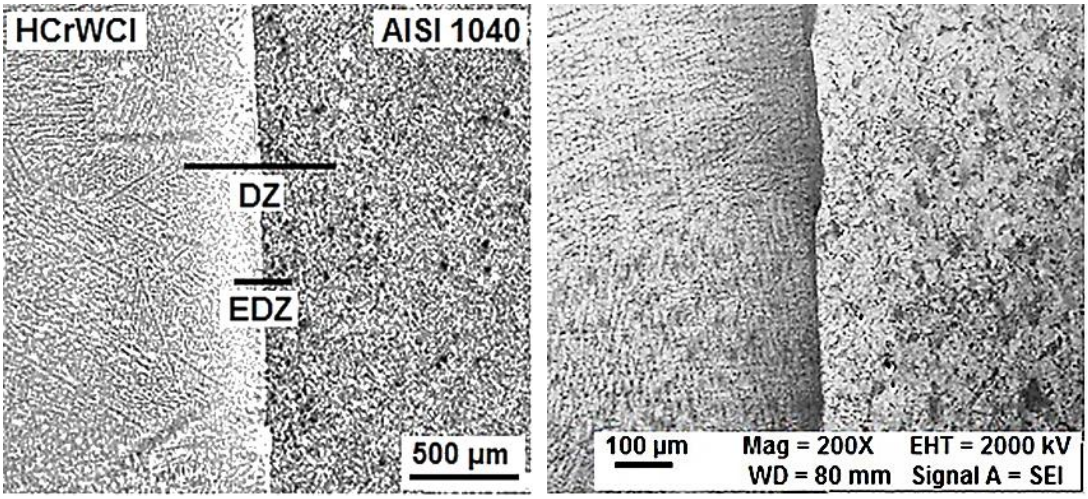

Figure 3. Optical and SEM photograph of S3 sample.

3.3. Phase analysis and weld metal chemical composition

The X-Ray analysis of the S3 welded sample is shown in Fig. 4. Phase and compounds such as Fe, $Cr_{23}C_6$, Cr_7C_3, CrC, Fe_3C were determined in the analyses. These metal carbides formed had a hard and brittle structure due to their ceramic character. Carbon, which is the dominant element of the diffusion process, was decisive in the emergence of the carbide layer. The carbide layer contained $Cr_{23}C_6$ and a metastable $C_{r7}C_3$ phase. Because, C and Cr reacted easily in FW of HCrWCI to AISI 1040 and formed carbides in the weld metal. EDS analysis of S3 sample is given in Fig. 5. The temperature at the welding interfaces was higher in S2 and S3 samples due to the increasing rotational speed. Since temperature was a driving force for diffusion, increased heat input with high friction time and rotational rate raised diffusion of Cr, C, Mn, Mo, Si and Ni elements in the weld zone.

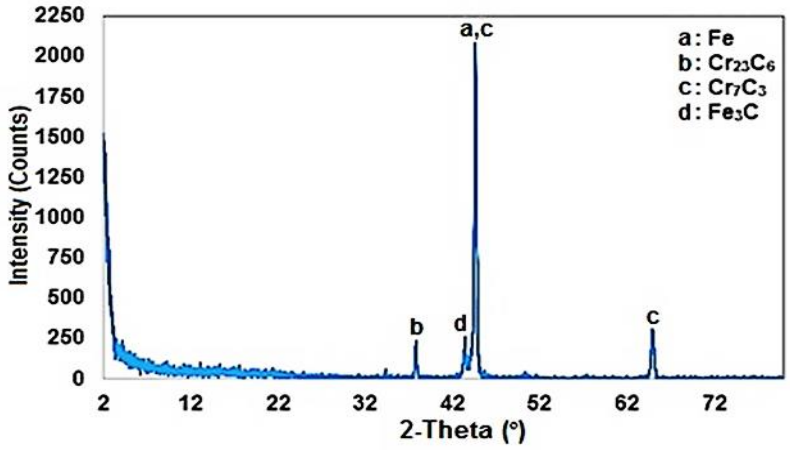

Figure 4. X-Ray analysis of S1 sample.

However, as we moved towards the base metal, the element diffusion decreased. It was determined that the original elemental percentages of the main materials were approached. Due to the differences in the chemical composition of the parent materials and the high heat during the joint operation, elemental diffusion formed. The more pronounced changes of C and Cr at the joint interface are presented in Fig. 5. Since the diffusion coefficient of Cr is much lower than C, there is no visible Cr content at the weld interface. Carbon was effective in the element diffusion process [19].

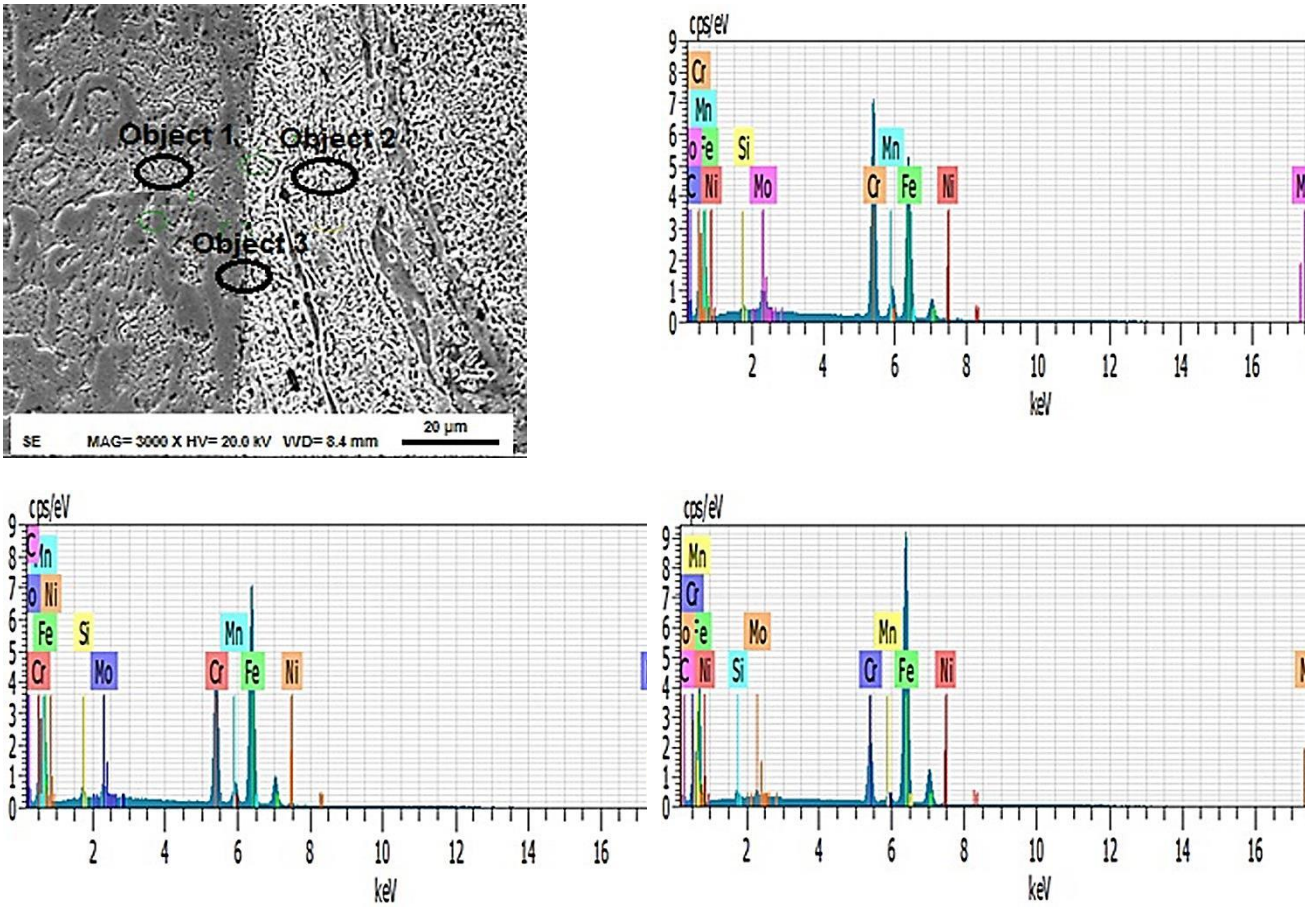

Figure 5. EDS analysis results of S3 sample.

Broken surface elemental mapping analysis of joint interface of S3 sample is given in Fig. 6. The transition of Cr, C, Mo, Ni, Si and Mn elements towards AISI1040 steel by HCrWCI occurred with plastic deformation and diffusion due to mechanical mixture. The iron element dominated the microstructure on the AISI1040 side as the main phase. It was determined that Cr, C, Mo, Si, Ni and Mn elements on the HCrWCI side diffused to the AISI 1040 side. The distribution of alloying elements such as Fe, Cr, C, Mo, Si, Ni and Mn in the weld area differend from place to place. The carbide layer composed of CrC and $Cr_{23}C_6$ formed at the weld interface due to element dispersal. Since the Cr is the most important active element in the chemical composition of HCrWCI, formation of chromium carbides in the microstructure was predictable. The major active element in the chemical content of HCrWCI was chromium. Therefore, chromium carbide formation was expected in the microstructure. The brittle cleavage fracture morphology was exhibited in the samples.

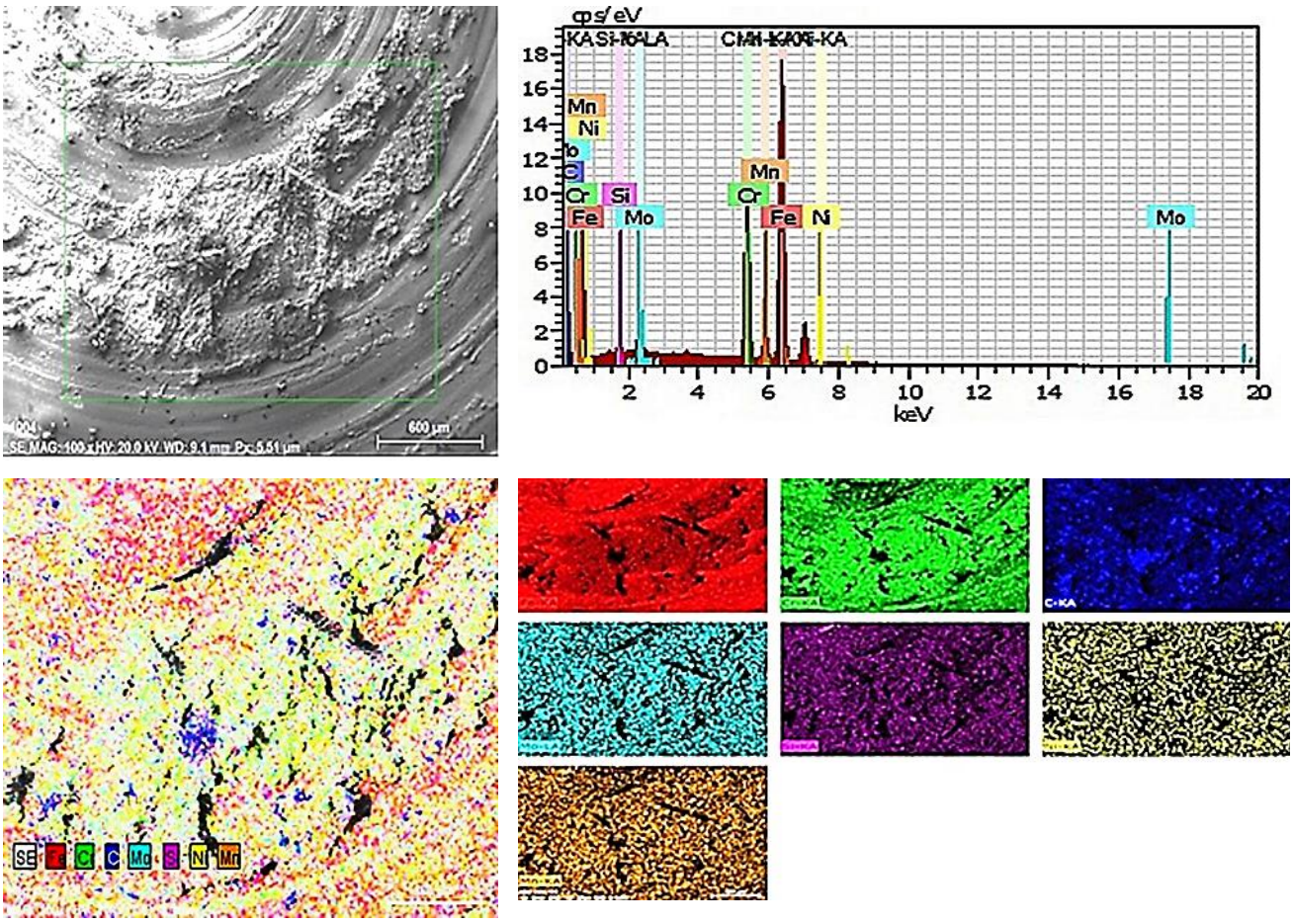

Figure 6. Broken surface elemental mapping analysis of S3 sample.

4. Conclusions

Mild carbon steel and HCrWCI are joined by friction welding under different joint conditions. The microstructures analysis of the weld interfaces, fracture morphology, presence and distribution of elements on joint zone were analyzed. The main conclusions are summarized as follows.

A rotation speed of 1600 rpm was not exactly sufficient for joining AISI 1040-HCrWCI alloys, but a rotation speed of 1800 rpm was adequate.

The rotational speed from the FW process parameters had a significant impact on the quality of the welded joint.

As stated in the literature, it was determined that four different regions were formed in welded joints.

Significant differences were detected in the quantities of flanges formed with increasing rotational period.

Due to the differences in the chemical composition of the parent materials and the high heat during the joint operation, elemental diffusion formed.

The carbides composed of Cr_7C_3 and $Cr_{23}C_6$ formed at the weld interface due to element dispersal.

Carbon was effective in the element diffusion leading to the formation of the carbides.

The brittle cleavage fracture morphology was exhibited in the samples.

Acknowledgment

This work, ADYU was supported by the Scientific Research Project Unit under the project number (MÜFYL/2018-001).

Conflicts of interest

The authors state that did not have conflict of interests

References

[1] Paventhan R., Lakshminarayanan P., Fatigue behaviour of friction welded medium carbon steel and austenitic stainless steel dissimilar joint, *Mater. Des.*, 32(4) (2011) 1888–1894.

[2] Arivazhagan N., Senthilkumaran K., Narayanan S., Devendranath Ramkumar K., Surendra S., Prakash S., Hot corrosion behavior of friction welded AISI4140 and AISI 304 in K_2SO–60% NaCl mixture, *J. Mater. Sci. Tech.*, 28(10) (2012) 895–904.

[3] Muralimohan C.H., Muthupandi V., Sivaprasad K., Properties of friction welding titanium stainless steel joints with a nickel interlayer, *Procedia Mater. Sci.*, 5 (2014) 1120–1129.

[4] Madhusudhan R.G., Role of nickel as an interlayer in dissimilar metal friction welding of maraging steel to low alloy steel, *J. Mater. Proces. Tech*., 212(1) (2012) 66–77.

[5] Çelik S., Ersözlü İ., Investigation of the mechanical properties and microstructure of friction welded joints between AISI4140 and AISI1050 steels, *Mater. Des.*, 30(4) (2008) 970–976.

[6] Damodaram R., Raman S., Rao P.K., Microstructure and mechanical properties of friction welded alloy 718, *Mater. Sci. Eng.*, 560 (2013) 781–786.

[7] Lippold J.C, Kotecki D.J., Welding metallurgy and weldability of stainless steels, New Jersey: John Wiley, (2005).

[8] Yin Y., Yang X., Cui L., Cao J., Xu W., Microstructure and mechanical properties of underwater friction taper plug weld on X65 steel with carbon and stainless steel plugs, *Sci. Technol. Weld. Join.*, 21 (4) (2016) 259–266.

[9] Li W., Vairis A., Preuss M., Ma T., Linear and rotary friction welding review, *Int. Mater. Rev.*, 61(2) (2016) 71–100.

[10] Ma H., Qin G., Geng P., Li F., Fu B., Meng X., Microstructure characterization and properties of carbon steel to stainless steel dissimilar metal joint made by friction welding, *Mater. Des.*, 86 (2015) 587–597.

[11] Suresh D., Meshram G., Madhusudhan R., Friction welding of AA6061 to AISI4340 using silver interlayer, *Defence Tech.*, 11(3) (2015) 292–298.

[12] Kumar R., Alasubramanian M., Experimental investigation of Ti6Al4V titanium alloy and 304L stainless steel friction welded with copper interlayer, *Defence Tech.*, 11(1) (2015) 65–75.

[13] Soysal T., Effect of solidification models on predicting susceptibility of carbon steels to solidification cracking, *Weld. World*., (2021) 1-12. https://doi.org/10.1007/s40194-021-01132-0

[14] Azizieh M., Khamisi M., Lee D.J.,. Yoon E.Y, Kim H.S., Characterizations of dissimilar friction welding of ST37 and CK60 steels, *Int. J. Adv. Manuf. Technol.* 85 (2016) 2773–2781.

[15] Winiczenko R., Effect of friction welding parameters on the tensile strength and microstructural properties of dissimilar AISI 1020-ASTM A536 joints, *Int. J. Adv. Manuf. Technol.*, 84 (2016) 941–955.

[16] Mortensen K. S., Jensen C.G., Conrad L.C., Losee F., Mechanical properties and microstructures of intertia friction welded 416 stainless steel, *Weld. J.*, 80 11, (2001) 268–273.

[17] Kalsi N.S., Sharma V.S., A statistical analysis of rotary friction welding of steel with varying carbon in workpieces, *Int. J. Adv. Manuf. Technol.*, 57 (2011) 957–967.

[18] Kimura M., Kasuya K., Kusaka M., Kaizu K., Fuji A., Effect of friction welding condition on joining phenomena and joint strength of friction welded joint between brass and low carbon steel, *Sci. Technol. Weld. Join.*, 14(5) (2009) 404–412.

[19] Teker T., Karakurt E.M., Ozabacı M., Güleryüz Y., Investigation of weldability of AISI 304 and AISI 1030 steels welded by friction welding, *Metal. Res. Tech.*, 117(6) (2020) 601–609.